PHYSICAL REVIEW B **90**, 214517 (2014)

Electronic structure of $LaO_{1-x}F_xBiSe_2$ ($x = 0.18$) revealed by photoelectron spectromicroscopy

N. L. Saini,[1] D. Ootsuki,[2] E. Paris,[1,3] B. Joseph,[1,4] A. Barinov,[4] M. Tanaka,[5] Y. Takano,[5] and T. Mizokawa[1,2,6]
[1] *Dipartimento di Fisica, Universitá di Roma "La Sapienza," Piazzale Aldo Moro 2, 00185 Roma, Italy*
[2] *Department of Physics, University of Tokyo, 5-1-5 Kashiwanoha, Chiba 277-8561, Japan*
[3] *Center for Life NanoScience@Sapienza, Istituto Italiano di Tecnologia, Viale Regina Elena 291, 00185 Rome, Italy*
[4] *Elettra Sincrotrone Trieste S.C.p.A., Area Science Park, 34012 Basovizza, Trieste, Italy*
[5] *National Institute for Materials Science, 1-2-1 Sengen, Tsukuba 305-0047, Japan*
[6] *Department of Complexity Science and Engineering, University of Tokyo, 5-1-5 Kashiwanoha, Chiba 277-8561, Japan*

(Received 16 October 2014; revised manuscript received 30 November 2014; published 19 December 2014)

We report an electronic structure study on $LaO_{1-x}F_xBiSe_2$ ($x = 0.18$) by means of photoelectron spectromicroscopy. The Fermi surfaces and band dispersions are basically consistent with the band-structure calculations on BiS_2-based materials, indicating that the electron correlation effects may be irrelevant to describe physics of the new $BiSe_2$ system. In $LaO_{1-x}F_xBiSe_2$ ($x = 0.18$), the area of the Fermi pockets is estimated to be 0.16 ± 0.02 per Bi, consistent with the amount of F substitution. Although the spectromicroscopy technique avoids the effect of microscale inhomogeneity for angle-resolved photoemission spectroscopy (ARPES), the ARPES spectral features are rather broad in the momentum space, indicating the likely effect of local disorder in the $BiSe_2$ layer.

DOI: 10.1103/PhysRevB.90.214517 PACS number(s): 74.25.Jb, 74.70.−b, 79.60.−i, 71.20.−b

I. INTRODUCTION

Soon after the discovery of superconductivity in $Bi_4O_4S_3$ with the BiS_2 layer [1], a new family of BiS_2-based layered superconductors was identified with a composition of $REO_{1-x}F_xBiS_2$ (RE = rare-earth elements). Since then, the physical properties of these new materials have been studied by various experimental techniques [2–18]. In particular, the $REO_{1-x}F_xBiS_2$ system consists of the electronically active BiS_2 layers and the REO spacer layers, and the carrier concentration of the BiS_2 layers can be controlled by the F substitution in the spacer layers with superconducting transition temperature T_c depending on the size of the RE ion. The T_c value also depends on the growth procedure, and a maximum T_c of ~10.5 K appears in $LaO_{1-x}F_xBiS_2$ ($x = 0.5$) synthesized by high-pressure annealing [4]. In addition, T_c is highly susceptible to the external pressure, e.g., $LaO_{1-x}F_xBiS_2$ ($x = 0.5$) synthesized at ambient pressure annealing shows a T_c of ~2.5 K, while it increases rapidly to 10 K at ~1 GPa [11,12,16]. Very recently, Tomita *et al.* has found a maximum T_c of 10.7 K at ~0.7 GPa and has assigned this to be due to a structural phase transition from tetragonal to monoclinic at this pressure [18]. These experiments indicate that T_c in the BiS_2-based materials should be related to the structural instability of the BiS_2 layer.

Various studies have been carried out to alter the structural instability by substitutions in the electronically active BiS_2 layer with a hope to obtain higher T_c in these materials. Among these, substitution of sulphur by heavier chalcogen atoms has been promising; however, the $LaO_{1-x}F_xBiSSe$ [19] and $LaO_{1-x}F_xBiSe_2$ [20], with heavier chalcogen ions, exhibit superconductivity with $T_c \sim 3.8$ and ~ 2.6 K, respectively. It has been proposed that a larger buckling distortion of the $BiSe_2$ layer is responsible for the reduced T_c [21]. On the theoretical front, Usui *et al.* has proposed that a Fermi surface nesting of quasi-one-dimensional Bi $6p_x/p_y$ bands is responsible for the superconductivity [22]. On the other hand, Yildirim emphasized the roles of strong electron phonon coupling, where a zone center ferroelectric phonon mode and a $(q,q,0)$ phonon mode coupled with a charge density wave are expected to play a significant role at $x = 0$ and 0.5, respectively [23].

Very recently, an x-ray photoemission spectroscopy (XPS) study on $LaO_{1-x}F_xBiS_2$ [24] and angle-resolved photoemission spectroscopy (ARPES) studies on $NdO_{1-x}F_xBiS_2$ [25,26] have revealed that there is an overall agreement between the band-structure calculations and the experimental band dispersions and Fermi surfaces. However, the XPS spectral weight near the Fermi level (E_F) appears to disagree with the calculations, and the disagreement emphasizes the importance of the electron-electron and/or electron-phonon interactions [24]. The possible polaron correlation effect is also suggested by the peculiar temperature dependence reported in the ARPES study by Zeng *et al.* [25]. On the other hand, the ARPES study by Ye *et al.* indicates rather weak electron correlations [26]. In addition, an optical spectroscopy study by Wang *et al.* excludes strong electron/polaron correlations [27]. The conflicting conclusions between the ARPES and optical studies suggest that the polaron correlation may be enhanced at the surface and that the surface electronic states are modified with respect to the bulk electronic states. Interestingly, nanoscale stripe patterns have been observed at the cleaved surface of $NdO_{1-x}F_xBiS_2$ by means of scanning tunneling microscopy [28], indicating that the cleaved surface of $REO_{1-x}F_xBiS_2$ may suffer from structural and electronic reconstructions. The disagreement between the two ARPES studies [25,26] would be related to a kind of microscale phase separation (or microscale coexisting domains) between two phases, with and without the nanoscale reconstruction of the cleaved surfaces. Another serious problem is that the area of the observed Fermi surfaces is much smaller than that expected from the amount of the F substitution in the previous works on the BiS_2 system [25,26]. The large deviation from the expected Fermi surfaces may indicate charge redistribution at the cleaved surface, which would affect the interpretation of the ARPES results. In this context, ARPES studies on related systems including $LaO_{1-x}F_xBiSe_2$ would be useful to resolve the issues on the electron and/or polaron correlation effect and the deviation on the Fermi surface area. In addition, space-resolved ARPES with submicrometer spatial resolution would be helpful to address the issue on the microscale phase separation of the cleaved surfaces.

In the present work, we focus on $LaO_{0.82}F_{0.18}BiSe_2$, of which single crystals have been recently grown by Tanaka *et al.* [21]. The main purpose of this study is to verify by photoelectron spectromicroscopy if microscale electronic inhomogeneity exists on the cleaved surface of the new $BiSe_2$ system. This is followed by measurements of Fermi surfaces and band dispersions using submicrometer beam size on the best part of the cleaved surface and compare the outcome with the reported results on the BiS_2-based systems. The spectromicroscopy reveals microscale inhomogeneity related to the surface LaO layer and enables ARPES measurements, avoiding the effect of the microscale electronic inhomogeneity due to the submicrometer spatial resolution. The Fermi surfaces and band dispersions are basically consistent with the band-structure calculations; however, the experimental features are relatively broad, suggesting possible nanoscale lattice disorder.

II. EXPERIMENT

The single crystals were grown as reported by Tanaka *et al.* [21]. The photoelectron spectromicroscopy results were obtained at the spectromicroscopy beamline, Elettra synchrotron facility, Trieste [29]. Photons at 27 eV were focused through a Schwarzschild objective in order to obtain a submicrometer-size beam spot. For the present measurements, the total energy resolution was set to about 50 meV and the angle resolution was 0.35 degree. The scanning photoemission spectromicroscopy images were obtained in the step size of 10 μm for the overview image and 1 μm for the fine image. The single crystals were oriented by *ex situ* Laue measurements and were cleaved *in situ* at 37 K under ultrahigh vacuum at 10^{-10} Torr. All the measurements were performed at the same temperature of 37 K. A standard photoemission microscopy procedure was used to remove topographic features from the images presented [30].

III. RESULTS AND DISCUSSION

Figure 1(a) shows a photoelectron spectromicroscopy image of the cleaved surface of $LaO_{0.82}F_{0.18}BiSe_2$ in which photoemission intensity was integrated from 0.5 to –3.5 eV relative to E_F. The regions with different contrast and brightness are mainly derived from large height difference in the cleaved surface. Although some regions appeared as very dark or very bright in the overview image in Fig. 1(a), the cleaved surface showed the moderately bright region with reasonably good flatness. The moderately bright region of Fig. 1(a) was selected as indicated by the solid box, and a fine image of 100 μm × 100 μm was taken as shown in Fig. 1(b). There is no appreciable electronic inhomogeneity in the fine image of photoemission intensity integrated from 0.5 to –3.5 eV. Figure 1(c) shows photoemission spectra at the three points (A, B, and C) selected from the fine image of Fig. 1(b). Interestingly, the photoemission spectral shape at point A is different from those at points B and C. The photoemission intensity from–1.0 to –2.0 eV, which is derived from the Se $4p$ (and Bi $6s$) states of the $BiSe_2$ layer, is relatively strong at point A. On the other hand, the peak at ~ -2.3 eV, which corresponds to the O $2p$ band from the LaO layer as will be discussed later, is enhanced at points B and C. When the photoemission intensity was integrated from–1.0 to –2.0 eV, the upper part of the fine image gets brighter than the lower part, as displayed in Fig. 1(d). The difference in the O $2p$ band indicates microscale inhomogeneity of the cleaved surface that would be related to the surface LaO layer. Therefore, it is reasonable to judge that point A, with less O $2p$ intensity, is more suitable than points B and C for probing the bulk electronic structure. The spectromicroscopy technique allowed us to select the relatively homogeneous region (at least in the microscale) from the inhomogeneous surface.

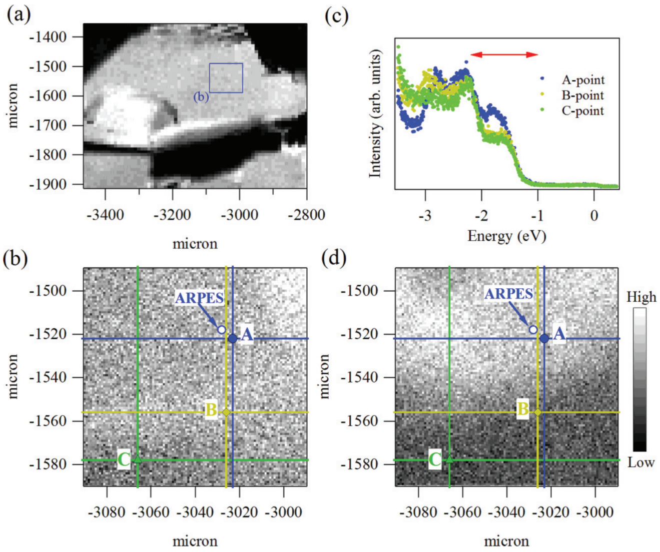

FIG. 1. (Color online) (a) Overview image of photoelectron spectromicroscopy on $LaO_{0.82}F_{0.18}BiSe_2$. The photoemission intensity is integrated from 0.5 to –3.5 eV relative to E_F. The solid box indicates the region selected for the fine image. (b) Fine image of photoelectron spectromicroscopy on $LaO_{0.82}F_{0.18}BiSe_2$. The photoemission intensity is integrated from 0.5 to –3.5 eV relative to E_F. (c) Photoemission spectra taken at points A, B, and C in Fig. 1(b). (d) Fine image of photoelectron spectromicroscopy on $LaO_{0.82}F_{0.18}BiSe_2$. The photoemission intensity is integrated from–1.0 to –2.0 eV relative to E_F.

Figure 2(a) shows the Fermi surface map measured at 37 K around point A in Fig. 1(d). Here, k_x (or k_y) is the momentum along the Γ-X direction or the Bi-Bi direction of the $BiSe_2$ plane. The Fermi surface map shows ARPES intensity integrated within ±10 meV above and below the Fermi level (E_F). The map was obtained by tetragonal symmetrization of the ARPES intensity measured in the region indicated by the dotted box. The solid square centered at Γ represents the two-dimensional Brillouin zone of the $BiSe_2$ plane. The relationship between k_x and k_z (momentum perpendicular to the $BiSe_2$ plane) at $h\nu = 27$ eV is shown in Fig. 2(b) for reasonable inner potential values of 13, 14, and 15 eV. At this photon energy, the observed Fermi surfaces are roughly located around the X point in the Brillouin zone. The rectangular Fermi pockets around the X point were clearly observed, consistent with the ARPES works on $NdO_{1-x}F_xBiS_2$ [25,26].

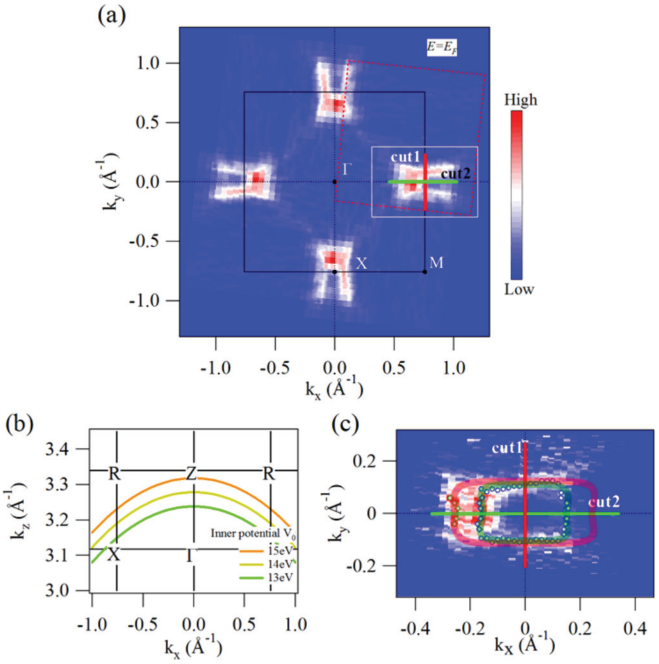

FIG. 2. (Color online) (a) Fermi surface map at $h\nu = 27$ eV of $LaO_{0.82}F_{0.18}BiSe_2$. The dotted box indicates the region in which the ARPES data were taken. The map is obtained by tetragonal symmetrization. The image in the dotted box was rotated by 90°, 180°, and 270° around Γ, and the ARPES intensity was averaged when the rotated boxes overlap. (b) Relationship between k_x and k_z at $h\nu = 27$ eV. (c) Fermi pockets around the X point. The open circles indicate peaks in MDCs that correspond to E_F crossing points.

Figure 2(c) shows the zoom of the Fermi pockets around the X point. The open circles indicate peaks in momentum distribution curves (MDCs) at E_F that correspond to E_F crossing points. Two Fermi pockets with rectangular shape were identified as illustrated by the solid curves in Fig. 2(c). The areas of the two Fermi pockets were estimated to be 5.94% and 9.25% of the two-dimensional Brillouin zone. Assuming good two dimensionality, the area of the Fermi pockets should correspond to the electron concentration in the $BiSe_2$ or BiS_2 layer introduced by the F substitution. The electron concentration was estimated to be $\sim 0.16 \pm 0.02$ per Bi in $LaO_{0.82}F_{0.18}BiSe_2$, which is larger than 0.07 per Bi for $NdO_{0.7}F_{0.3}BiS_2$ [25] and is comparable to 0.16 per Bi for $NdO_{0.5}F_{0.5}BiS_2$. [26] The estimated electron concentration is consistent with that expected from the nominal composition in $LaO_{0.82}F_{0.18}BiSe_2$, indicating that the present ARPES result represents the bulk electronic structure. On the other hand, the deviation from the nominal value is substantially large in $NdO_{1-x}F_xBiS_2$, and the substantial reduction of the electron concentration from the nominal value is attributed to Bi defects [26]. If the Bi defects are responsible for the large deviation in $NdO_{1-x}F_xBiS_2$, it is interesting to note that the $LaO_{1-x}F_xBiSe_2$ system with fewer Bi defects tends to show lower T_c than $NdO_{1-x}F_xBiS_2$. Another possibility is that the previous ARPES results on $NdO_{1-x}F_xBiS_2$ would be affected by surface reconstruction. In either case, the present work on $LaO_{0.82}F_{0.18}BiSe_2$ provides the first ARPES result consistent with the bulk electronic structure of the ideal $BiSe_2$ layer.

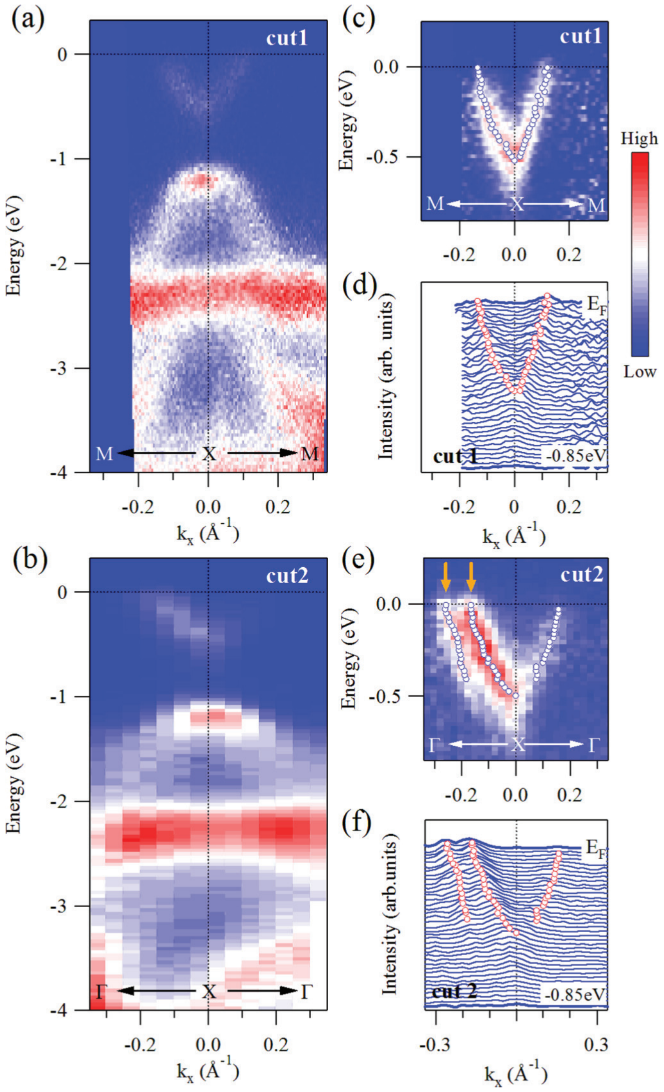

FIG. 3. (Color online) (a) Second derivative plot for the wide energy range along cut 1 of Fig. 2(c). (b) Second derivative plot for the wide range along cut 2 of Fig. 2(c). (c) Second derivative plot for the near E_F range along cut 1. (d) MDCs for the near E_F range along cut 1. (e) Second derivative plot for the near E_F range along cut 2. (f) MDCs for the near E_F range along cut 2. The open circles indicate peaks in MDCs that correspond to band dispersions. k_x is the momentum relative to the X point.

Figure 3(a) shows the band dispersions along cut 1 of Fig. 2(c). In Fig. 3(a), $-d^2\rho(E)/dE^2$ was smoothed and plotted as a function of k_y, where $\rho(E)$ is the ARPES spectrum and E is the energy relative to E_F. The conduction bands crossing E_F can be attributed to the Bi $6p$ bands, while the other low-lying bands (valence bands) are mainly derived from the Bi $6s$ and Se $4p$ orbitals in the $BiSe_2$ layer and the O $2p$ orbitals in the LaO layer. As shown in Fig. 3(a), the flatband at ~ -2.3 eV is very peculiar and is not reproduced by the band-structure calculations. The peculiar flatband is also reported in $NdO_{0.5}F_{0.5}BiS_2$ [26] and can be attributed to the O $2p$ band of the LaO or NdO layer. Figure 3(b) shows the band dispersions along cut 2 of Fig. 2(c). Here, $-d^2\rho(E)/dE^2$ was smoothed and plotted as a function of k_x. Again the flatband

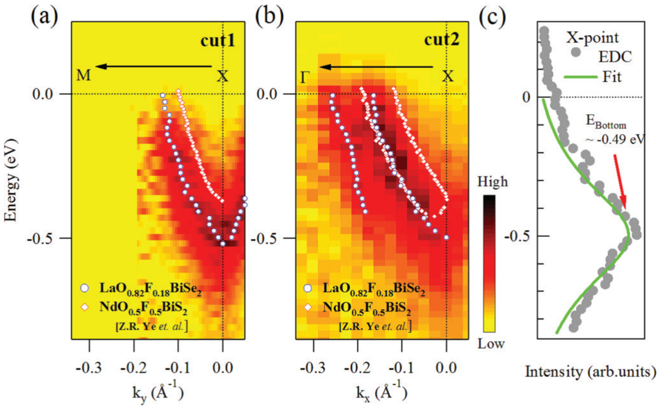

FIG. 4. (Color online) (a) Comparison between the band dispersions along cut 1 estimated for $LaO_{0.82}F_{0.18}BiSe_2$ compared with the band dispersions reported for $NdO_{0.5}F_{0.5}BiS_2$ [26]. (b) Comparison between the band dispersions along cut 2 estimated for $LaO_{0.82}F_{0.18}BiSe_2$ compared with the band dispersions reported for $NdO_{0.5}F_{0.5}BiS_2$ [26]. k_x is the momentum relative to the X point. (c) EDC at the X point and Gaussian fit.

at ∼−2.3 eV is clearly observed and can be assigned to the O $2p$ band of the LaO layer. The bottom of the Bi $6p$ bands at the X point is ∼–0.5 eV, while the top of the Bi $6s$/Se $4p$ bands is located at ∼–1.2 eV. The energy gap between the Bi $6p$ conduction bands and the Bi $6s$/Se $4p$ valence bands is 0.7 eV, which is slightly smaller than that of $NdO_{0.7}F_{0.3}BiS_2$ and $NdO_{0.5}F_{0.5}BiS_2$ [25,26].

As for the Bi $6p$ band dispersions near E_F, the ARPES intensity and MDCs along cut 1 [cut 2] are displayed in Figs. 3(c) and 3(d) [Figs. 3(e) and 3(f)], respectively. The open circles indicate peaks in the MDCs at each energy and roughly correspond to band dispersions along cuts 1 and 2. Along cut 1 of Fig. 2(c), the Bi $6p$ bands cross E_F at $k_y \sim 0.13$ Å^{-1}. The Bi $6p$ bands are split into the two branches along cut 2. The branches cross E_F at $k_x \sim 0.17$ and 0.24 Å^{-1}, respectively, as indicated by the arrows in Fig. 3(d). Here, k_x is the momentum relative to the X point. In this direction, the spin-orbit splitting of the Bi $6p$ bands can be well resolved, supporting the existence of the two Fermi pockets in Fig. 2(c). The E_F crossing points are consistent with the estimation of the Fermi surface area in the previous paragraph, although the substantial broadening in the momentum space does not allow precise estimation. Interestingly, the broad ARPES features in the momentum space indicate that large atomic disorder in the $BiSe_2$ layer is likely. Since the ARPES signals are derived from the region without the microscale electronic inhomogeneity, the broadening can be attributed to nanoscale inhomogeneity, which is probably related to the larger buckling and local lattice distortion of the $BiSe_2$ layer.

The observed Bi $6p$ band dispersions qualitatively agree with the band-structure calculations and the ARPES results on the BiS_2 system [25,26]. As shown in Figs. 4(a), 4(b), and 4(c), the bottom of the Bi $6p$ bands are located at ∼0.5 eV below E_F in $LaO_{0.82}F_{0.18}BiSe_2$, while it is around ∼0.4 eV below E_F in $NdO_{0.5}F_{0.5}BiS_2$ [26] and ∼0.35 eV below E_F in $NdO_{0.7}F_{0.3}BiS_2$ [25]. The hump observed in the Bi $6p$ bands in $NdO_{0.7}F_{0.3}BiS_2$ [25] is absent in $LaO_{1-x}F_xBiSe_2$. There can be several possible reasons for the absence of the hump structure. One possibility is that the electron-phonon interaction responsible for the hump gets weaker in going from the BiS_2 to the $BiSe_2$ systems. Another possible reason could be the differences in the surface quality of the two systems. Apparently, the surface quality of the $BiSe_2$ is very good, and the results obtained here indeed represent the bulk band structure. This is also because the present ARPES results were obtained for the best region of the cleaved surface by means of the spectromicroscopy technique with submicrometer spatial resolution.

IV. CONCLUSION

In summary, we have studied the electronic structure of $LaO_{1-x}F_xBiSe_2$ ($x = 0.18$) by means of photoelectron spectromicroscopy. The spectromicroscopy image indicates a homogeneous distribution of the electronic state with the absence of any electronic inhomogeneity at a submicrometer scale. The ARPES spectral features, measured on the homogeneous part of the cleaved surface using submicrometer resolution, are rather broad in the momentum space, probably due to some local (nanoscale) lattice disorders in the $BiSe_2$ layer. The Fermi surfaces and band dispersions are basically consistent with the band-structure calculations, suggesting that the electron/polaron correlations are irrelevant in the $BiSe_2$ systems.

ACKNOWLEDGMENTS

The authors thank the Elettra staff for their cooperation during the experiments. The present work is a part of the collaboration between Sapienza University of Rome, the University of Tokyo, and NIMS, Tsukuba. The work is partly supported by a Grant-in-Aid for Scientific Research from the Japan Society for Promotion of Science. The work at Sapienza is partially supported by PRIN2012 (Grant No. 2012X3YFZ2).

---

[1] Y. Mizuguchi, H. Fujihisa, Y. Gotoh, K. Suzuki, H. Usui, K. Kuroki, S. Demura, Y. Takano, H. Izawa, and O. Miura, Phys. Rev. B **86**, 220510(R) (2012).

[2] S. K. Singh, A. Kumar, B. Gahtori, G. Sharma, S. Patnaik, and V. P. S. Awana, J. Am. Chem. Soc. **134**, 16504 (2012).

[3] Y. Mizuguchi, S. Demura, K. Deguchi, Y. Takano, H. Fujihisa, Y. Gotoh, H. Izawa, and O. Miura, J. Phys. Soc. Jpn. **81**, 114725 (2012).

[4] H. Kotegawa, Y. Tomita, H. Tou, H. Izawa, Y. Mizuguchi, O. Miura, S. Demura, K. Deguchi, and Y. Takano, J. Phys. Soc. Jpn. **81**, 103702 (2012).

[5] J. Xing, S. Li, X. Ding, H. Yang, and H.-H. Wen, Phys. Rev. B **86**, 214518 (2012).

[6] B. Li, Z. W. Xing, and G. Q. Huang, Europhys. Lett. **101**, 47002 (2013).

[7] K. Deguchi, Y. Mizuguchi, S. Demura, H. Hara, T. Watanabe, S. J. Denholme, M. Fujioka, H. Okazaki, T. Ozaki, H. Takeya,

T. Yamaguchi, O. Miura, and Y. Takano, Europhys. Lett. **101**, 17004 (2013).

[8] S. Demura, Y. Mizuguchi, K. Deguchi, H. Okazaki, H. Hara, T. Watanabe, S. J. Denholme, M. Fujioka, T. Ozaki, H. Fujihisa, Y. Gotoh, O. Miura, T. Yamaguchi, H. Takeya, and Y. Takano, J. Phys. Soc. Jpn. **82**, 033708 (2013).

[9] V. P. S. Awana, Anuj Kumar, Rajveer Jha, Shiva Kumar Singh, Anand Pal, Shruti, J. Saha, and S. Patnaik, Solid State Commun. **157**, 21 (2013).

[10] R. Jha, A. Kumar, S. K. Singh, and V. P. S. Awana, J. Appl. Phys. **113**, 056102 (2013).

[11] D. Yazici, K. Huang, B. D. White, A. H. Chang, A. J. Friedman, and M. B. Maple, Philos. Mag. **93**, 673 (2013).

[12] D. Yazici, K. Huang, B. D. White, I. Jeon, V. W. Burnett, A. J. Friedman, I. K. Lum, M. Nallaiyan, S. Spagna, and M. B. Maple, Phys. Rev. B **87**, 174512 (2013).

[13] H. Lei, K. Wang, M. Abeykoon, E. S. Bozin, and C. Petrovic, Inorg. Chem. **52**, 10685 (2013).

[14] X. Wan, H. C. Ding, S. Y. Savrasov, and C. G. Duan, Phys. Rev. B **87**, 115124 (2013).

[15] J. Lee, M. B. Stone, A. Huq, T. Yildirim, G. Ehlers, Y. Mizuguchi, O. Miura, Y. Takano, K. Deguchi, S. Demura, and S.-H. Lee, Phys. Rev. B. **87**, 205134(R) (2013).

[16] C. T. Wolowiec, D. Yazici, B. D. White, K. Huang, and M. B. Maple, Phys. Rev. B **88**, 064503 (2013).

[17] J. Kajitani, K. Deguchi, T. Hiroi, A. Omachi, S. Demura, Y. Takano, O. Miura, and Y. Mizuguchi, J. Phys. Soc. Jpn. **83**, 065002 (2014).

[18] T. Tomita, M. Ebata, H. Soeda, H. Takahashi, H. Fujihisa, Y. Gotoh, Y. Mizuguchi, H. Izawa, O. Miura, S. Demura, K. Deguchi, and Y. Takano, J. Phys. Soc. Jpn. **83**, 063704 (2014).

[19] X.-C. Wang, D.-Y. Chen, Q. Guo, J. Yu, B.-B. Ruan, Q.-G. Mu, G.-Fu. Chen, and Z.-A. Ren, arXiv:1404.7562.

[20] A. Krzton-Maziopa, Z. Guguchia, E. Pomjakushina, V. Pomjakushin, R. Khasanov, H. Luetkens, P. K. Biswas, A. Amato, H. Keller, and K. Conder, J. Phys.: Condens. Matter **26**, 215702 (2014).

[21] M. Tanaka, M. Nagao, Y. Matsushita, M. Fujioka, S. J. Denholme, T. Yamaguchi, H. Takeya, and Y. Takano, J. Solid State Chem. **219**, 168 (2014).

[22] H. Usui, K. Suzuki, and K. Kuroki, Phys. Rev. B **86**, 220501(R) (2012).

[23] T. Yildirim, Phys. Rev. B. **87**, 020506(R) (2013).

[24] S. Nagira, J. Sonoyama, T. Wakita, M. Sunagawa, Y. Izumi, T. Muro, H. Kumigashira, M. Oshima, K. Deguchi, H. Okazaki, Y. Takano, O. Miura, Y. Mizuguchi, K. Suzuki, H. Usui, K. Kuroki, K. Okada, Y. Muraoka, and T. Yokoya, J. Phys. Soc. Jpn. **83**, 033703 (2014).

[25] L. K. Zeng, X. B. Wang, J. Ma, P. Richard, S. M. Nie, H. M. Weng, N. L. Wang, Z. Wang, T. Qian, and H. Ding, Phys. Rev. B **90**, 054512 (2014).

[26] Z. R. Ye, H. F. Yang, D. W. Shen, J. Jiang, X. H. Niu, D. L. Feng, Y. P. Du, X. G. Wan, J. Z. Liu, X. Y. Zhu, H. H. Wen, and M. H. Jiang, Phys. Rev. B **90**, 045116 (2014).

[27] X. B. Wang, S. M. Nie, H. P. Wang, P. Zheng, P. Wang, T. Dong, H. M. Weng, and N. L. Wang, Phys. Rev. B. **90**, 054507 (2014).

[28] T. Machida, Y. Fujisawa, M. Nagao, S. Demura, K. Deguchi, Y. Mizuguchi, Y. Takano, and H. Sakata, J. Phys. Soc. Jpn. **83**, 113701 (2014).

[29] P. Dudin, P. Lacovig, C. Fava, E. Nicolini, A. Bianco, G. Cautero, and A. Barinov, J. Synchrotron Rad. **17**, 445 (2010).

[30] M. Marsi, L. Casalis, L. Gregoratti, S. Gunther, A. Kolmakov, J. Kovac, D. Lonza, and M. Kiskinova, J. Electron Spectrosc. Relat. Phenom. **84**, 73 (1997).